SVD-VLC: A novel capacity maximizing VLC MIMO system architecture under illumination constraints

P.M. Butala, H. Elgala, T.D.C. Little
Department of Electrical and Computer Engineering
Boston University, Boston, Massachusetts
{*pbutala,helgala,tdcl*}*@bu.edu*

December 16, 2013

MCL Technical Report No. 12-16-2013

Abstract–Multiple-input multiple-output (MIMO) systems using multiple light emitting diode (LED) sources and photo-diode (PD) detectors are attractive for visible light communication (VLC) as they offer a capacity gain proportional to the number of parallel single-input single-output (SISO) channels. MIMO VLC systems exploit the high signal-to-noise ratio (SNR) of a SISO channel offered due to typical illumination requirements to overcome the capacity constraints due to limited modulation bandwidth of LEDs. In this work, a modified singular value decomposition VLC (SVD-VLC) MIMO system is proposed. This system maximizes the data rate while maintaining the target illumination and allowing the channel matrix to vary in order to support mobility in a practical indoor VLC deployment. The upper bound on capacity of the proposed SVD-VLC MIMO system is calculated assuming an imaging receiver. The relationship between the proposed system performance and system parameters total power constraint, lens aperture and random receiver locations are described.

In *Globecom 2013 Workshop on Optical Wireless Communications (GC13 WS - OWC)*, Atlanta, December 2013. This work was supported by the Engineering Research Centers Program of the National Science Foundation under NSF Cooperative Agreement No. EEC-0812056.

1 Introduction

In VLC technology, the indoor solid-state lighting infrastructure is used to provide the required room illumination and optical wireless access simultaneously [1]. Illumination grade LEDs offer low modulation bandwidths and relatively high radiant flux. Thus under typical illumination conditions (400 lx), a SISO VLC channel operates at low bandwidth and high SNR. The throughput of the SISO channel can be increased by implementing spectrally efficient modulation schemes. The capacity of the channel can be increased by improving the modulation bandwidth of the LEDs. Another way of increasing the capacity of the channel is by implementing MIMO techniques that distribute the signalling power budget among multiple simultaneous SISO links. Capacity of AWGN communication channels increases linearly with SNR at low SNR and logarithmically with SNR at high SNR. Thus, the aggregate sum of the capacities of each link operating at low SNR can be greater than the capacity of the SISO channel operating at high SNR.

Schemes such as blue filtering [2], equalization [3] and multiple resonated LEDs [4] are proposed to extend the LED 3dB modulation bandwidth. Complex modulation schemes such as orthogonal frequency-division multiplexing (OFDM) or discrete multi-tone modulation (DMT) have been proposed to improve the spectral efficiency of the SISO VLC channel and increase its throughput [5–8].

A spatial multiplexing indoor MIMO technique for VLC technology using OFDM and a non-imaging receiver is considered in [9]. However, the non-imaging receiver suffers from outages at symmetry points [10]. Angle diversity receivers [11] help improve the system coverage. However these receivers are bulky and impractical to incorporate in hand-held devices. Imaging receivers help decorrelate the MIMO channel matrix coefficients and offer significant improvements in system performance [12]. The imaging receiver architecture [13] has the potential to provide the highest capacity for a VLC channel while being incorporated in a hand-held device.

MIMO schemes implementing the native SVD architecture are used in RF communications to optimally utilize the capacity of the channel when the channel state information (CSI) is known at the transmitter and receiver [14]. A hybrid system implementing the VLC channel as the high capacity downlink while providing illumination and another medium for the uplink to provide the CSI to the transmitter seems to be the accepted model and a reasonable assumption [15].

An SVD architecture for MIMO VLC communications is proposed in [16]. The authors define an aggregate sum of the average flux emitted from multiple LEDs as the upper bound for the radiated optical flux in order to fulfill the eye safety requirements. Given this system, it is possible to violate the eye safety requirements if the channel matrix is not full rank. Also, the illumination profile generated by the system transitions to a different state every time the channel matrix changes. Finally, the solution restricts itself to M-ary pulse amplitude modulation (PAM) and necessitates different optimization for different modulation schemes.

In this work, the SVD-VLC system for diffuse indoor MIMO VLC channel is proposed. We show how to calculate an upper bound on the capacity of the channel using an imaging receiver. Also introduced is a novel method to maintain illumination and the concept of dedicated illumination streams (I1 streams) and information + illumination streams (I2 streams). This concept achieves and maintains the illumination targets while supporting

mobility, i.e. variable channel matrix. An imaging receiver is considered to decorrelate the coefficients of the MIMO channel matrix. For sake of completeness, the spectral power distribution (SPD) of the LED sources, the filter transmission across all wavelengths of interest and the PD responsivity curve is considered in the analysis.

The following notations are used in this paper. Regular font indicates a scalar. Bold font indicates a vector or a matrix. $\mathbf{A}^*$ indicates conjugate transpose of $\mathbf{A}$. Operators $:=$, $E[.]$, $M[.]$, $||.||$ indicate defination, expectation and element-by-element multiplication and euclidean norm in that order. $sgn(.)$ is the signum function.

The remainder of this paper is organized as follows. A brief introduction of the VLC SISO channel is provided in Section II. Computation of the MIMO channel matrix using an imaging receiver is shown in Section III. The SVD-VLC MIMO system to generate and maintain requested illumination profile is then proposed in Section IV. In Section V, the effect of changing system parameters on system performance is analyzed using simulation results for an example setup. Conclusions are drawn in Section VI.

2 SISO Channel

In this section, a SISO VLC link with additive white gaussian noise (AWGN) is introduced and its capacity under unbiased signal power constraint K and LED bandwidth B is computed. Let x be the emitted radiant signal flux, y be the received signal current after the optical-to-electrical conversion, $w \sim \mathcal{N}(0, \sigma^2_{SISO})$ be the channel noise and h be the overall channel gain which includes the responsivity of the PD. The SISO channel model is then given as

$$y = hx + w \tag{1}$$

Figure 1 illustrates coordinate systems used in the analysis. $[\hat{\mathbf{X}}\ \hat{\mathbf{Y}}\ \hat{\mathbf{Z}}]$ and $[\hat{\mathbf{x}}\ \hat{\mathbf{y}}\ \hat{\mathbf{z}}]$ are the basis vectors for the global coordinate system (GCS) and the receiver's coordinate systems (RCS). A corner of the room is the origin of the GCS while the centroid of the aperture of the receiver is set as the origin of RCS. The receiver's basis vectors are assumed always parallel to the length, width and surface normal of the sensor.

Let $[x_{tx}\ y_{tx}\ z_{tx}]$ be the location of centroid (C_{tx}) of the illumination surface of the transmitter and $[x_{rx}\ y_{rx}\ z_{rx}]$ be the location of the centroid of the receiver concentrator surface in the GCS. The optical axis is then given by (2a). The transmitter is then located at height $\mathbf{d}^z$ above the receiver in RCS given by (2b)

$$\mathbf{d} = \begin{bmatrix} x_{tx} \\ y_{tx} \\ z_{tx} \end{bmatrix} - \begin{bmatrix} x_{rx} \\ y_{rx} \\ z_{rx} \end{bmatrix} \tag{2a}$$

$$\mathbf{d}^z = (\mathbf{d}.\hat{\mathbf{z}})\hat{\mathbf{z}} \tag{2b}$$

Let the radiant intensity emitted by the transmitter at any angle ϕ subtended between the transmitter surface normal and the optical axis be given by $L(\phi)$. Radiant intensity of a lambertian transmitter of order m is given by

$$L(\phi) = \begin{cases} \frac{(m+1)}{2\pi} cos^m(\phi) & ; -\pi/2 \leq \phi \leq \pi/2 \\ 0 & ;\ \text{else} \end{cases} \tag{3}$$

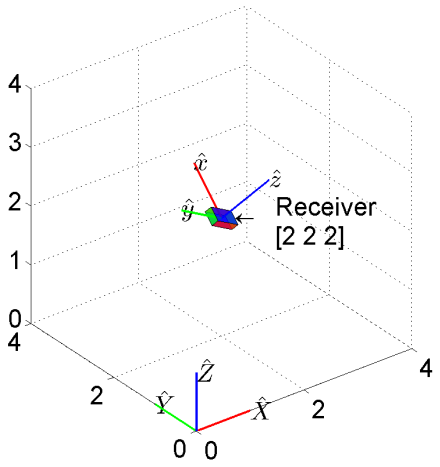

Figure 1: Illustration of the coordinate systems used

The SISO receiver comprises of a filter, an optical concentrator and a PD. Let ψ be the angle between the receiver surface normal ($\hat{\mathbf{z}}$) and the optical axis. Let η be the refractive index of the material of the concentrator and ψ_c be the field of view of the concentrator. Then the optical concentrator gain is given by

$$G(\psi) = \begin{cases} \frac{\eta^2}{sin^2(\psi_c)} & ; 0 \leq \psi \leq \psi_c \leq \frac{\pi}{2} \\ 0 & ; \psi > \psi_c \end{cases} \tag{4}$$

Let $S(\lambda)$ be the normalized SPD of the emitted radiant flux such that area under curve is 1W. Let $R(\lambda)$ be the responsivity of the PD. Let the transmission of the filter be $T(\psi, \lambda)$. Thus the effective responsivity of the receiver including the transmission and gains from all optical components is given by

$$R_e(\psi) = G(\psi) \int_{\lambda_{min}}^{\lambda_{max}} S(\lambda) T(\psi, \lambda) R(\lambda) d\lambda \tag{5}$$

where λ_{min} to λ_{max} span all the wavelengths of interest.

If A is the active area of the PD, the overall channel gain h is then given by

$$h = L(\phi) \frac{A}{||\mathbf{d}||^2} cos(\psi) R_e(\psi) \tag{6}$$

In a typical SISO VLC link, shot noise from ambient illumination dominates over that from signal [17]. Let q be the charge of an electron. Worst cast shot noise from isotropic ambient radiant flux $P_a(\lambda)$ is given by

$$\sigma_{sh}^2 = \frac{2qAG(\psi_c)}{\psi_c} \int_{\lambda_{min}}^{\lambda_{max}} \int_0^{\psi_c} P_a(\lambda) R(\lambda) T(\psi, \lambda) d\psi d\lambda \tag{7}$$

The transimpedance amplifier (TIA) is generally the first current to voltage amplifier stage after the PD. In the absence of significant ambient illumination, the TIA noise is the dominant source of noise [18]. Thus shot noise from signal itself is ignored. The thermal noise from the TIA is considered as the dominant electronic noise component and is given by [18],

$$\sigma_{th}^2 = \frac{4kT}{R_f} \tag{8}$$

where k is the Boltzmann's constant, T is the absolute temperature and R_f is the feedback resistance of the TIA.

Thus the total noise current density is given by

$$\sigma_{SISO}^2 = \sigma_{sh}^2 + \sigma_{th}^2 \tag{9}$$

Using Shannon's capacity formula for a AWGN baseband channel with a transmitter constrained to power K independent of illumination and bandwidth B, the upper bound on capacity of the SISO VLC channel is given by [19]

$$C_{SISO} = log_2 \left(1 + \frac{h^2 K}{\sigma_{SISO}^2 B} \right) \tag{10}$$

3 Imaging MIMO Channel Matrix

In this section, an imaging MIMO system as illustrated in Figure 2 is considered. Multiple (N_{tx}) luminaires are located near the ceiling of the indoor space to provide illumination and act as transmitter(s) for communication. The imaging receiver uses the imaging optics to decorrelate the optical MIMO channel matrix coefficients to achieve parallel links in a cross-talk free configuration. It comprises of the optics and a sensor. The sensor is made of a number (N_{px}) of contiguous pixels each made up of a filter and a PD as optical detector. The imaging MIMO channel is described as

$$\mathbf{Y} = \mathbf{HX} + \mathbf{W} \tag{11}$$

where $\mathbf{X}$ is a N_{tx} dimensional vector whose each element is the radiant signal flux emitted by each transmitter. $\mathbf{Y}$ is a N_{px} dimensional vector whose each element is the output signal current from each pixel. $\mathbf{H}$ is a N_{px} x N_{tx} dimensional channel gain matrix where each element or channel gain coefficient h_{ij} indicates the net channel gain from transmitter j to pixel i. $\mathbf{W}$ is a N_{px} dimensional noise vector. For imaging receivers, the shot noise at each pixel due to ambient illumination is severely diminished [12] and thus TIA input noise current is dominant source of noise [18]. Thus for imaging receivers, $\mathbf{W} \sim \mathcal{N}(\mathbf{0}, \sigma^2_{MIMO}\mathbf{I})$ where σ_{MIMO} equals input noise current density of the TIA.

For each individual link, the free space gain is defined as the ratio of the radiant flux incident at the aperture of the receiver to that of the from the transmitter j. Let $[x_j\ y_j\ z_j]$ be the location of centroid C_j of the illumination surface of the j^{th} transmitter and $[x_{rx}\ y_{rx}\ z_{rx}]$ be the location of the centroid of the receiver aperture in (2a). Let A_o be the area of the aperture opening. The free space channel gain is then given by

$$h_j^{fs} = L_j(\phi_{ij})\frac{A_o}{||\mathbf{d}_j||^2}cos(\psi_{ij}) \tag{12}$$

Let f be the focal length of the imaging optics and d_j be the length of the optical axis between the transmitter j and the receiver. ψ_c^{rx} is the field of view (FOV) of the receiver. Depending on the sensor dimensions, this may be smaller than or equal to the FOV of

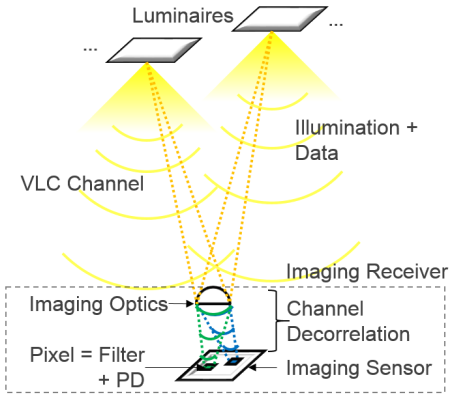

Figure 2: Imaging MIMO VLC system

imaging optics ψ_c^o. The magnification of the imaging optics is given by

$$M = \begin{cases} \frac{f}{||\mathbf{d}_j^z|| - f} & ; \psi_j \leq \psi_c^{rx} \\ 0 & ; \psi_j > \psi_c^{rx} \end{cases} \tag{13}$$

Assuming the receiver is focused on the transmitter, the location of C_j as projected in the RCS is given by

$$\begin{bmatrix} x_{sp} \\ y_{sp} \\ z_{sp} \end{bmatrix}_j = \begin{bmatrix} -M(\mathbf{d_j}.\hat{\mathbf{x}}) \\ -M(\mathbf{d_j}.\hat{\mathbf{y}}) \\ -f \end{bmatrix} \tag{14}$$

Assuming the mathematical model of the shape of the luminaire's illumination surface is known, the shape of its projected spot on the plane of surface of the sensor can be calculated. Depending on the geometry of the transmitters and receiver, a pixel may receive light from multiple spots. Accordingly, the system performance gets severely degraded due to the correlated channel matrix coefficients and inter channel interference (ICI).

Non-polygonal shapes can be approximated to a polygon with very small error. Polygon itersection algorithms can be used to compute the shared area between a spot and pixel. The imaging channel gain (15) between transmitter j and pixel i is then given by the ratio of the fraction of the area of the spot j that is incident on pixel i to total area of the spot j.

$$h_{ij}^{im} = \frac{\text{Area}(\text{spot}_j \cap \text{pixel}_i)}{\text{Area}(\text{spot}_j)} \tag{15}$$

Let $S_j(\lambda)$ be the SPD of the flux over link j and $T_i(\lambda)$ and $R_i(\lambda)$ be the filter transmission and responsivity at pixel i respectively. The optical filter transmission in this case is assumed independent of the angle of incidence of the flux. Let Q be the transmission of the imaging optics. The effective responsivity of pixel i over link j is given by

$$R_{ij} = Q \int_{\lambda_{min}}^{\lambda_{max}} S_j(\lambda) T_i(\lambda) R_i(\lambda) d\lambda \tag{16}$$

Thus the net channel gain matrix $\mathbf{H}$ can be computed from the free space channel gain, the imaging channel gain and effective pixel responsivity by

$$\mathbf{H}(i,j) = h_{ij} = h_j^{fs} h_{ij}^{im} R_{ij} \tag{17}$$

where element h_{ij} is the net channel gain from transmitter j to pixel i.

4 SVD-VLC Framework

The SVD technique applies coordinate system transformations on correlated channels and generates simultaneous independent links and maximizes the capacity of the MIMO channel. Native SVD does not impose any form of non-negativity or illumination constraint. The SVD-VLC architecture is derived from the native SVD architecture to optimally utilize the capacity of the channel while satisfying illumination constraints.

As described in previous section, the MIMO VLC channel model is given by (11). The channel matrix $\mathbf{H}$ can be decomposed into rotation and scaling matrices using SVD as

$$\mathbf{H} = \mathbf{U}\mathbf{\Lambda}\mathbf{V}^* \tag{18}$$

$\mathbf{U}$ and $\mathbf{V}$ are unitary rotation matrices while $\mathbf{\Lambda}$ is a diagonal scaling matrix. Matrices $\mathbf{H}$ and $\mathbf{\Lambda}$ have the same rank $\Gamma \leq min(N_{tx}, N_{px})$. The diagonal elements of $\mathbf{\Lambda}$ $(\lambda_1 ... \lambda_k ... \lambda_\Gamma)$ are the singular values of matrix $\mathbf{H}$. Now let us define new variables in rotated coordinate systems as

$$\mathbf{X}^{'} := \mathbf{V}^*\mathbf{X} \tag{19a}$$

$$\mathbf{Y}^{'} := \mathbf{U}^*\mathbf{Y} \tag{19b}$$

$$\mathbf{W}^{'} := \mathbf{U}^*\mathbf{W} \tag{19c}$$

Inserting the above definitions in (11) and then premultiplying both sides by $\mathbf{U}^*$ transforms the MIMO channel model as

$$\mathbf{Y}^{'} = \mathbf{\Lambda}\mathbf{X}^{'} + \mathbf{W}^{'} \tag{20}$$

$\mathbf{X}^{'}$ and and $\mathbf{Y}^{'}$ is the input and output for the transformed system. Elements of $\mathbf{W}^{'}$ will be i.i.d and have the same variance as $\mathbf{W}$ [14]. The transformed simultaneous independent

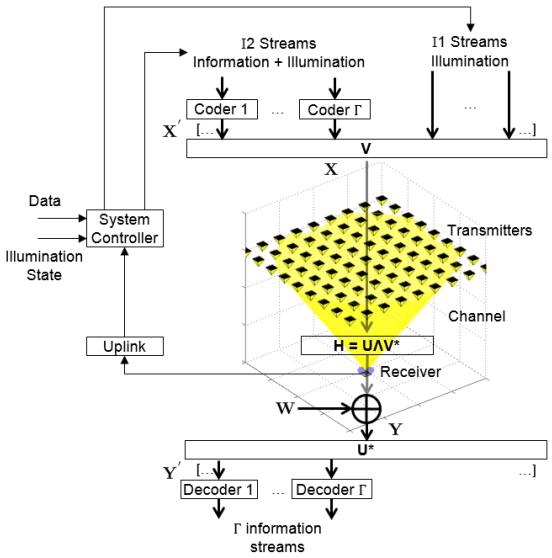

Figure 3: SVD-VLC System Block Diagram

link models are described by

$$y_k^{'} = \lambda_k x_k^{'} + w_k^{'}; 1 \leq k \leq N_{tx} \tag{21}$$

In the above model, the information streams are defined over inputs $x_k^{'}$. Note $\lambda_k = 0; k > \Gamma$ and thus no information can be transmitted over those links. At the transmitters, transformation $\mathbf{V}$ multiplexes the streams over the physical channel. At the receiver, transformation $\mathbf{U}^*$ demultiplexes the independent streams. These transformations are also called pre-processing and post-processing.

For indoor VLC system, information is carried over an intensity signal which cannot be negative. (22) implies that input symbols $\mathbf{X}^{'}$ should be defined to generate positive values after preprocessing.

$$\mathbf{X} \geq \mathbf{0} \leftrightarrow \mathbf{V}\mathbf{X}^{'} \geq \mathbf{0} \tag{22}$$

In an indoor space, a user can specify a desired illumination state. This sets each element of $\mathbf{P}$ as the average radiant flux to be emitted by each luminaire. (23) specifies this constraint over the original and transformed channels.

$$E[\mathbf{X}] = \mathbf{P} \leftrightarrow \mathbf{P}^{'} = E[\mathbf{X}^{'}] = \mathbf{V}^*\mathbf{P} \tag{23}$$

Note that each $x_k^{'}$ must maintain the average signal at $P_k^{'}$ even if the transformed channel gain $\lambda_k = 0; k > \Gamma$. One way of achieving this is by setting $x_k^{'} = P_k^{'}; k > \Gamma$. So even though links carry no information, it is vital to satisfy the average signal constraint to service illumination.

The above two constraints together specify a range of values that the $x_k^{'}$ symbols can take and this is given by

$$M[\mathbf{X}^{'}.sgn(\mathbf{P}^{'})] \geq \mathbf{0} \tag{24}$$

Figure 3 illustrates SVD-VLC system architecture. The 'I1-streams' are the $N_{tx} - \Gamma$ links that service only illumination. The 'I2-streams' are the Γ information + illumination bearing links. The I1 and I2 streams are preprocessed by $\mathbf{V}$ to transform and multiplex them over the channel. This multiplexing generates and maintains the desired illumination state in the indoor space. At the imaging receiver, the TIAs for each pixel add i.i.d white gaussian noise to each link. Postprocessing by $\mathbf{U}^*$ demultiplexes the parallel links and recovers the Γ I2 streams. The streams can be jointly decoded to optimally recover the transmitted data.

Given an aggregate signal power budget K, the waterfilling algorithm [20] specifies the optimal signal power allocation for each independent parallel link. Let this be given by $K_k^{'}$ independent of illumination for each transformed link where $\sum_{k=1}^{\Gamma} K_k^{'} = K$. The upper bound on capacity of the MIMO VLC channel with imaging receiver can then be calculated as

$$C_{SVD-VLC} = \sum_{k=1}^{\Gamma} log_2 \left(1 + \frac{\lambda_k^2 K_k^{'}}{\sigma_{MIMO}^2 B}\right) \tag{25}$$

Table 1: Configuration Parameters

Parameter		Value	Units
Room Length	L_{rm}	4	m
Room Width	W_{rm}	4	m
Room Height	H_{rm}	4	m
Transmiter grid pitch[1]	D_{tx}	0.5	m
Total number of transmitters[1]	N_{tx}^{L} x N_{tx}^{W}	9x9	-
Transmitter Lambertian Order	m	1	-
Optics Field of View	ψ_c^o	60	degrees
Optics focal length[1]	f	5	mm
Optics transmission[1]	Q	1	-
Concentrator refractive index[2]	η	1.5	-
Ideal filter transmission	$T(\lambda)\forall\lambda$	1	-
Sensor Side length	a_{rx}	5	mm
Pixel side length[1]	α_{rx}	1	mm
Pixel pitch[1]	δ_{rx}	1	mm
Total number of pixels[1]	N_{px}^{L} x N_{px}^{W}	5x5	-
Responsivity	$R(\lambda)\forall\lambda$	0.4	A/W
Receiver bandwidth	B	50	MHz
TIA noise current density	I_{pa}	5	pA/$\sqrt{\text{Hz}}$

[1] MIMO specific parameter
[2] SISO specific parameter

5 Results

The capacity bound of the MIMO channel with imaging receiver is analyzed and compared with that of an equivalent SISO channel using an example simulation setup. Table 1 outlines the system parameters used. For the MIMO channel, the luminaires are arranged in a grid

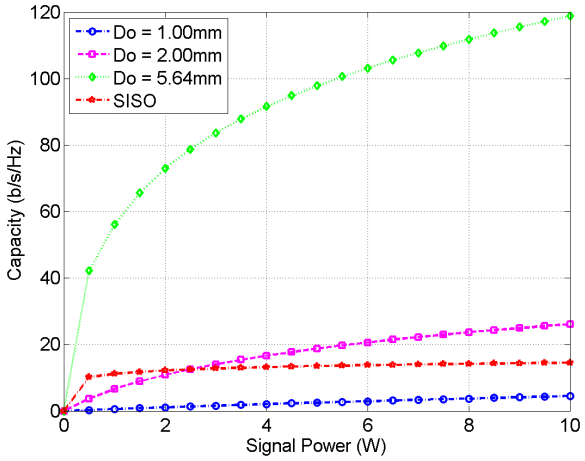

Figure 4: Capacity vs Power

Table 2: Simulation Illumination Constraints

Case	**Dominant luminaire(s)**	**400lx Setpoint location**
a	[1;3;3]	[1;3;1]
b	[3;1;3]	[3;1;1]
c	[1;1;3] and [3;3;3]	[2;2;1]

Table 3: Simulation Results

Receiver		**Simulated illumination (lx)**		
Location	**Rank(H)**	**a**	**b**	**c**
[1.6 0.6 1.0]'	16	399.99	400.29	400.22
[2.8 0.4 1.4]'	12	400.00	401.75	400.00
[0.2 0.8 1.0]'	12	399.81	399.92	401.26
[1.2 1.4 1.6]'	9	400.06	400.01	401.97

at the a height of 3m in the room and a pitch of D_{tx}. The luminaires are assumed to be point sources with sufficient output luminous flux to provide the desired illumination. The SPD of the emitted flux is approximated using sum of gaussians to that used in [2]. The receiver bandwidth is assumed to be 50 MHz [3]. For this analysis the receiver is always assumed located at the center of the length-width plane. The same sensor side length a_{rx} is maintaied for the SISO PD and the imaging receiver. The case where the aperture collection area of the imaging receiver is the same as the area of the SISO receiver is also considered.

Figure 4 shows the theoretical capacity of the SISO and MIMO channels over a range of signal power constraints and different lens aperture diameters when the receiver is at the center of the 1m plane. The capacity of the MIMO VLC channel is then calculated at the same power constraints as a SISO channel. As expected, the capacity of the imaging channel does increase with increasing aperture diameter. At aperture diameter of 5.64mm, the imaging receiver and the SISO receiver collect the same amount of average radiant flux, however the MIMO channel shows huge spectral efficiency gains. This gain in capacity can be explained by the introduction of multiple parallel links due to the imaging receiver architecture and the reduction in ambient shot noise per channel as indicated in [12]. While the imaging receiver collects the same amount of ambient flux as the SISO receiver, this flux can be assumed to be equally divided among all the pixels on the receiver due to imaging optics. Thus each link has greatly reduced ambient flux, thus reducing the noise and improving the capacity. The limiting factor in this case is the thermal noise.

To illustrate generation and maintenance of an illumination state using the SVD-VLC architecture, three different scenarios for different illumination states were simulated using SVD-VLC. For these scenarios, Table 2 outlines the illumination constraints. The dominant luminaire(s) column specifies the transmitter(s) whose average output radiant flux was configured to be 20x that as compared to each of the other transmitters. Setpoint location column specifies the location in the room where 400lx illumination is requested. The combination of these two values specifies a unique illumination state for each scenario. The constraints were specified in this manner to prevent an unacceptably high illumination level at any other point on the illumination surface. A more complex illumination state can be im-

posed as a constraint to generate a particular light field, however this simple case is sufficient to illustrate the SVD-VLC behavior.

Receiver locations at four different time instants are chosen pseudorandomly to simulate a varying channel matrix due to mobility. For each of the three scenarios, a 1024 bit long data sequence is generated from a uniformly distributed pseudorandom number sequence in the (0,1) range. The data sequence is scaled to meet the average signal constraint specified by $\mathbf{P}^{'}$ and I1 and I2 streams are generated. After multiplexing these streams over the physical channel, the resulting illumination state is calculated as illustrated in Figure 5. Table 3 shows values for the illumination achieved at the setpoint location as the channel matrix varies with the receiver's location. It can be seen that despite the variations in the channel matrix, the illumination state remains nearly constant.

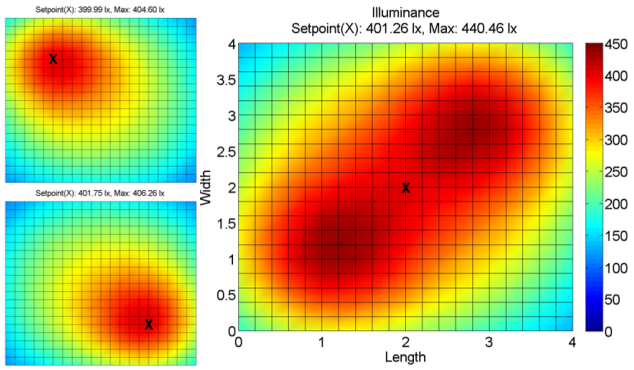

Figure 5: Generation and maintenance of illumination state by SVD-VLC. 'X' marks the setpoint location in the illumination plane at 1m height. Scenarios: (a) Top left (b) Bottom left (c) Right

6 Conclusion

The SVD-VLC architecture is introduced to implement MIMO VLC channel with an imaging receiver while maintaining illumination. Upper bound on capacity for an instance of the MIMO VLC system using SVD-VLC architecture is calculated and compared with that of an equivalent SISO channel under different signal power constraints. It is shown that for the same received radiant flux, MIMO channel with imaging receiver offers large capacity gains over the equivalent SISO channel. Additionally, the concept of using I1 and I2 streams to transmit information without affecting illumination is introduced. It is also shown that the system can achieve and maintain a user defined illumination state under changing channel conditions. SVD-VLC system does require the CSI to be known at the transmitter and receiver. While it may be possible in a pseudo-static indoor scenario to acquire this information with minimal resource overhead, it does add complexity to the system.

7 Acknowledgement

This work was supported primarily by the Engineering Research Centers Program of the National Science Foundation under NSF Cooperative Agreement No. EEC-0812056.

References

[1] H. Elgala, R. Mesleh, and H. Haas, "Indoor optical wireless communication: potential and state-of-the-art," *Communications Magazine, IEEE*, vol. 49, no. 9, pp. 56–62, 2011.

[2] J. Grubor, S. Randel, K.-D. Langer, and J. Walewski, "Broadband information broadcasting using led-based interior lighting," *Lightwave Technology, Journal of*, vol. 26, no. 24, pp. 3883–3892, 2008.

[3] L. Zeng, D. O'brien, H. Le-Minh, K. Lee, D. Jung, and Y. Oh, "Improvement of date rate by using equalization in an indoor visible light communication system," in *Circuits and Systems for Communications, 2008. ICCSC 2008. 4th IEEE International Conference on*, 2008, pp. 678–682.

[4] H. L. Minh, D. O'Brien, G. Faulkner, L. Zeng, K. Lee, D. Jung, and Y. Oh, "High-speed visible light communications using multiple-resonant equalization," *Photonics Technology Letters, IEEE*, vol. 20, no. 14, pp. 1243 –1245, july15, 2008.

[5] J. Vucic, C. Kottke, S. Nerreter, A. Buttner, K.-D. Langer, and J. W. Walewski, "White light wireless transmission at 200+ mb/s net data rate by use of discrete-multitone modulation," *Photonics Technology Letters, IEEE*, vol. 21, no. 20, pp. 1511 –1513, oct.15 2009.

[6] R. Mesleh, R. Mehmood, H. Elgala, and H. Haas, "Indoor mimo optical wireless communication using spatial modulation," in *Communications (ICC), 2010 IEEE International Conference on*, may 2010, pp. 1 –5.

[7] R. Mesleh, H. Elgala, and H. Haas, "An overview of indoor ofdm/dmt optical wireless communication systems," in *Communication Systems Networks and Digital Signal Processing (CSNDSP), 2010 7th International Symposium on*, july 2010, pp. 566 –570.

[8] S. Dissanayake, K. Panta, and J. Armstrong, "A novel technique to simultaneously transmit aco-ofdm and dco-ofdm in im/dd systems," in *GLOBECOM Workshops (GC Wkshps), 2011 IEEE*, dec. 2011, pp. 782 –786.

[9] A. Azhar, T. Tran, and D. O'Brien, "A gigabit/s indoor wireless transmission using mimo-ofdm visible-light communications," *Photonics Technology Letters, IEEE*, vol. 25, no. 2, pp. 171–174, 2013.

[10] L. Zeng, D. O'Brien, H. Minh, G. Faulkner, K. Lee, D. Jung, Y. Oh, and E. T. Won, "High data rate multiple input multiple output (mimo) optical wireless communications using white led lighting," *Selected Areas in Communications, IEEE Journal on*, vol. 27, no. 9, pp. 1654 –1662, december 2009.

[11] J. Carruthers and J. Kahn, "Angle diversity for nondirected wireless infrared communication," *Communications, IEEE Transactions on*, vol. 48, no. 6, pp. 960 –969, jun 2000.

[12] P. Djahani and J. Kahn, "Analysis of infrared wireless links employing multibeam transmitters and imaging diversity receivers," *Communications, IEEE Transactions on*, vol. 48, no. 12, pp. 2077–2088, 2000.

[13] J. Kahn, R. You, P. Djahani, A. Weisbin, B. K. Teik, and A. Tang, "Imaging diversity receivers for high-speed infrared wireless communication," *Communications Magazine, IEEE*, vol. 36, no. 12, pp. 88 –94, dec 1998.

[14] D. Tse and P. Viswanath, *Fundamentals of wireless communication*. New York, NY, USA: Cambridge University Press, 2005.

[15] M. Rahaim, A. Vegni, and T. D. C. Little, "A hybrid radio frequency and broadcast visible light communication system," in *GLOBECOM Workshops (GC Wkshps), 2011 IEEE*, 2011, pp. 792–796.

[16] K.-H. Park, Y. chai Ko, and M.-S. Alouini, "A novel power and offset allocation method for spatial multiplexing mimo systems in optical wireless channels," in *GLOBECOM Workshops (GC Wkshps), 2011 IEEE*, 2011, pp. 823–827.

[17] J. R. Barry, *Wireless Infrared Communications*. Norwell, MA, USA: Kluwer Academic Publishers, 1994.

[18] J. Kahn and J. Barry, "Wireless infrared communications," *Proceedings of the IEEE*, vol. 85, no. 2, pp. 265 –298, feb 1997.

[19] C. E. Shannon, "A mathematical theory of communication," *Bell System Technical Journal*, vol. 27, pp. 379–423 and 623–656, 1948.

[20] A. Goldsmith and P. Varaiya, "Capacity of fading channels with channel side information," *Information Theory, IEEE Transactions on*, vol. 43, no. 6, pp. 1986–1992, 1997.